Reviewer #1 Comments:

We thank the reviewer for the constructive comments. In the following, we repeat the reviewer's comments in black and insert our answers in blue. In some cases, we highlight the changes made in the manuscript, written in italic font whereas the original text is repeated with grey coloring.

This study estimates methane emissions in a key region where greenhouse gas emissions and satellite data have considerable biases. This uncertainty, along with the proportion of emissions from this region to the global burden, makes it a target for mitigation efforts. Regional emission estimates, therefore, are important in that direction. This manuscript is written concisely but needs some additional points. Key analysis to add includes a validation with independent data, as satellite data have been known to have biases in this region. Monsoon seasonality in emissions related to rain-fed agriculture or wetlands is expected, but how robust the estimate/conclusion should be shown with posterior statistics, with independent observations in this region. Also, the focus should be on the whole domain (the abstract also lacks that- e.g., what causes the seasonality for the whole domain), instead of projecting the LIB result as a key result. After addressing the comments, this manuscript may be considered for publication.

We thank the reviewer for this constructive comment and fully agree that validation with independent observations is, in principle desirable, particularly given the known challenges and potential biases of satellite methane retrievals over South Asia.

Independent validation

There is currently no publicly available dataset of ground-based observations for this region that we are aware of. To our knowledge, there is no data sets that are both (i) available for the study period and have good quality and (ii) have sufficiently regionally representative (not within an urban area) to provide a meaningful validation of our posterior emission estimates. Existing in-situ measurements in South Asia are extremely sparse and are often located in or near urban environments, making them poorly representative of the large-scale, predominantly agricultural and wetland emission regions that dominate our inversion domain. Much of in-situ data from the region is not openly accessible, limiting its use for independent validation.

To address this, now we have used the GOSAT-TROPOMI blended dataset (Balasus et al., 2023) to test our results. This dataset applies machine-learning-based bias correction and is developed independently of the WFMD TROPOMI retrievals used in our inversion. A new section now compares posterior model concentrations against this dataset, showing consistent seasonal behavior and improved agreement relative to the prior simulation. The corresponding figures and evaluation are provided at the end of this document for reference.

Robustness of posterior emissions

In addition to the sensitivity tests to the error assumptions, we now conducted sensitivity experiments by strongly perturbing prior flux magnitudes (~33–133 Tg CH_4 yr^{-1}). Despite these large changes, posterior emissions converge to a narrow range (~65–73 Tg CH_4 yr^{-1}) with consistent spatial and seasonal patterns. This indicates that the inversion is not strongly controlled by the absolute magnitude of the prior emissions and that the national-scale posterior estimates are relatively robust.

Domain-wide focus and seasonality

The processes driving the seasonality are different in different regions, and we therefore keep the separate discussions on the subregions. We believe that this is also an important validation aspect, since the seasonality can be understood in terms of run-off data for the different river basins. The fact that we do see different seasonality of methane emissions in the LIB, where the river flow is also driven by

snow melt, compared to the Bangladesh region, where the river flow is more directly controlled by the monsoon, corroborates the validity of our seasonal emission patterns.

Together these analyses indicate that our estimates are robust and the satellite observations provide meaningful constraint on methane emissions at the national scale for South Asia in 2020.

Specific points

Abstract

"Agriculture and wetlands contribute substantially to the regional budget,..". Better to be quantitative here. You have analyzed climatic factors in the South Asian domain as well. Better to reflect those aspects in the abstract also.

Agriculture and wetlands contribute substantially to the regional budget, with the flux increments coincident with rice-growing areas and inundated lowlands

We changed the text to:

Agriculture and wetlands contribute substantially to the regional budget, with the flux increments coincident with rice-growing areas and inundated lowlands. The largest positive emission increments of about 19.3 Tg occurring during the monsoon season (June–September), are consistent with enhanced rainfall and wetland inundation across the South Asian domain.

Introduction

26-27: "Methane (CH_4) is a potent greenhouse gas with a global warming potential 85 times higher than that of carbon dioxide over a 20-year period." Reference needed

Methane (CH_4) is a potent greenhouse gas with a global warming potential 85 times higher than that of carbon dioxide over a 20-year period.

Changed to:

Methane (CH_4) is a potent greenhouse gas with a global warming potential 84-87 times higher than that of carbon dioxide over a 20-year period (International Energy Agency, 2021).

59-60: include basic references for SCIAMACHY, GOSAT, etc., and give credit to the Agency behind the effort

The earliest satellite observations for methane were provided by the SCanning Imaging Absorption spectroMeter for Atmospheric CHartographY (SCIAMACHY) instrument onboard the ENVISAT satellite, launched in 2002. The launch of the first dedicated greenhouse gas monitoring satellite, GOSAT (Greenhouse Gases Observing Satellite), in 2009 opened the possibility for monitoring carbon dioxide and methane emissions across the globe. Since then, several other satellites have enhanced the GHG monitoring capabilities. The TROPOspheric Monitoring Instrument (TROPOMI) on the Sentinel-5 Precursor satellite, launched in October 2017, provides high-resolution, daily global observations of atmospheric methane. The TROPOMI data offer unprecedented spatial and temporal coverage well suited for GHG estimation both on global and regional scales.

Changed to:

The earliest satellite observations for methane were provided by the SCanning Imaging Absorption spectroMeter for Atmospheric CHartographY (SCIAMACHY) instrument onboard the European Space Agency's (ESA) ENVISAT satellite, launched in 2002 (Bovensmann et al., 1999). The launch of the first dedicated greenhouse gas monitoring satellite, GOSAT (Greenhouse Gases Observing Satellite) with its TANSO-FTS instrument developed by JAXA, in 2009 opened the possibility for monitoring carbon dioxide and methane emissions across the globe (Kuze et al., 2009). Since then, several other satellites have enhanced the GHG monitoring capabilities (Jacob et al., 2022). The TROPOspheric Monitoring Instrument (TROPOMI) on the ESA's Sentinel-5 Precursor satellite, launched in October 2017, provides high-resolution, daily global observations of atmospheric methane (Hu et al., 2016). The TROPOMI data offer unprecedented spatial and temporal coverage well suited for GHG estimation both on global and regional scales.

Connect the last two paragraphs of page 2 on the sparsity of surface networks to the use of satellites

Thank you for the comment, we joined the two paragraphs.

Also mention some studies on the biases in satellite products over Asia, then the biases in TROPOMI early products, and how this product is better.

Satellite retrievals of methane are known to have systematic biases that vary by instrument, retrieval methodology and region, driven by factors such as surface albedo, aerosols, and thin clouds. Over Asia, these effects have been shown to translate into substantial differences in inferred emissions, with GOSAT and TROPOMI based inversions differing by up to 7.7 Tg yr^{-1} over northern India and eastern China (Liang et al., 2023). Biases associated with surface reflectance, aerosol loading, and across-track striping in early TROPOMI products can exceed 10 ppb in some regions and have been linked to false methane anomalies caused by unmodelled surface spectral features or inadequate topographic information (Balasus et al., 2023; Jongaramrungruang et al., 2021; Lorente et al., 2023). Algorithm updates to the operational TROPOMI retrieval have substantially reduced albedo-dependent biases through improved spectroscopy, higher-resolution surface altitude data, and posteriori corrections (Lorente et al., 2021). The scientific TROPOMI WFMD product further addresses these issues by using higher-order polynomial fitting to better represent spectral albedo variability, updated digital elevation models, refined machine-learning based quality filtering, and orbit-wise destriping and calibration, resulting in reduced systematic errors and improved spatiotemporal consistency. Notably, persistent seasonal biases present in the operational product at high latitudes are largely absent in WFMD (Lindqvist et al., 2024; Schneising et al., 2023).

Data and methods

Section 2.2.

1. 126: Edgar > EDGAR

   Done!

2. 128: finn > FINN?

   Done!

3. How come the wetland prior map is so weak in Pakistan, while 10% of Pakistan's land is wetlands? Maybe use proper scales for each panel? Use non-linear scales for flux maps, as you will miss some key information.

This is not a matter of the flux scales. The wetland emissions in Pakistan are indeed very low (1 order less or even lower than in other places) in the prior inventories and do not appear in large scale as for Bangladesh. The bottom-up inventories estimate an emission of only **< 0.1 Tg/yr** of wetland emissions from Pakistan. In the recent study on wetland emissions by Chen et al., 2025, you can see the spatial distribution of wetland emissions as similar to our map.

4. 146: Significant landfill emissions can also be in other major cities. Maybe elaborate on other regions also.

   Notably high landfill emissions can also be found over the capital city of India, Delhi

   Changed to:

   "Notably regions of high landfill emissions can also be found over Islamabad, Delhi, Mumbai, Ahmedabad and Bangalore (Dogniaux et al., 2025; Toha et al., 2025)"

5. Table 1. Edgar > "EDGAR"

   Done!

Section 2.3.

1. Include reference to CAMS, EGG4, etc.

   Done!

2. ECMWF- write in full at the first use for all abbreviations (e.g. RMSD in line 166)

   Done!

Section 2.4

1. 169: Flexpart > FLEXPART

   Done!

Results

1. The prior map clearly shows emissions from anthropogenic sources in the LIB. So, how do the river discharge peaks correspond to methane emissions? If it is related to rain-fed agriculture, this should be clearly written with some references. (What is the agricultural practice in Pakistan etc.). Wetlands in Pakistan are also in the region where you have anthropogenic emissions (your wetland prior plot does not show that due to large emissions from Bangladesh). So the double peak, is it from seasonally inundated wetlands or seasonal agriculture?

   Both mechanisms are plausible. The inversion cannot tell us which mechanism is driving the emissions. We believe that the emissions are often due to the combination of both agricultural practices and wetland inundation, since both depend on precipitation and run-off. The emission peak in May could be driven by increased river-flow from snow melt and due to the onset of irrigated rice cultivation and the August peak with monsoon-driven inundation.

   There are basically two main agricultural seasons for Pakistan: Kharif and Rabi Seasons. Kharif crops require a lot of water to grow. For Kharif season, seeds are sowed from April-June and

harvested at the end of the monsoon. So, this could lead to emission in April-June. The second peak could be partly due to the monsoon driven inundation and partly from the agricultural conditions. No studies directly address the seasonal features of Pakistan's wetland inundation and agricultural practices.

2. Also, the aggregated posterior for SA also shows peaks in two seasons, as has been shown in some previous studies (e.g., Ganesan et al., 2017) for Indian agriculture emissions. So emphasis may be given to the whole domain instead of LIB.

   We agree that the aggregated posterior emissions over South Asia show clear seasonal peaks and that this domain-wide perspective is important. At the same time, we show the sub regional analyses because the processes driving methane seasonality differ across South Asia. Investigating subregions helps to interpret the underlying mechanisms. For example, the Lower Indus Basin (LIB) exhibits a seasonal pattern influenced partly by snowmelt-driven river discharge (Baig et al., 2022), whereas Bangladesh shows a stronger direct response to monsoon-driven inundation. The presence of physically consistent but distinct seasonal behavior across these regions supports the credibility of the inferred emission patterns.

3. Should mention in the Figure 10 caption about the prior uncertainty? How is the prior uncertainty calculated? Is it not small for South Asia?

   The prior inventories do not specify uncertainties. We have assumed them to be 100% of the prior fluxes on a grid cell level but with a lower limit of 1×10^{-9} kg m^{-2} h^{-1} ($2.8\text{x}10^{-13}$ kg m^{-2} s^{-1}). Prior error correlations are represented using an exponential decay function with a spatial correlation length of 250 km and a temporal scale of 30 days. The aggregated uncertainties are calculated as the root sum square of individual uncertainties. In the earlier calculations, the error cross-correlations were not considered when deriving uncertainties. Now we have included this, which leads to more realistic prior (66.3 ± 6.7 Tg yr^{-1}) and posterior uncertainty (73 ± 0.7 Tg yr^{-1}) estimates over South Asia. The smaller posterior uncertainty reflects the stronger constraint provided by the TROPOMI observations through the inverse calculation.

4. "However, since this validation is not against independent data, this shows only that the inversion is performing as expected". A posterior simulation with independent surface observation should be done, as satellite data are not real observations. So, make use of surface observations to demonstrate that the posterior fits well with observations in this region.

   In the absence of suitable surface observations, we validated the posterior simulation against the independent GOSAT–TROPOMI blended XCH_4 dataset (Balasus et al., 2023), which is developed independently of the WFMD retrievals used in this study.

5. Figure 11 gives the ensemble values, but where does it stand when compared to prior or recent studies? More information can be added there. Also, provide prior/posterior uncertainty in all applicable figures (e.g., no prior uncertainty in Figure 12, no posterior uncertainty in Figure 11).

   Prior estimate is 66.3 Tg ± 6.7 Tg yr^{-1}. We have now added the prior value in the figure 11 for easier comparison. Estimates from the recent studies were shown earlier in the introduction part as figure 1. Now we have moved this figure to the results part so that it is clear where our estimates stand compared to other studies.

   Thanks for pointing this out. Uncertainties are added to the figures. In figure 12, posterior ensemble standard deviation is shown with error bar, since prior flux is not perturbed here, there is no spread in prior values hence the error bar is not drawn there. Now, the prescribed prior uncertainty for the reference inversion is added as the error bar for prior fluxes.

6. Figure 12. Group the regions together (darker/lighter) for direct comparison to the respective prior.

   Thanks for the comment, we have now modified the figure.

7. 267-269: "The model prior mole fractions (orange line) significantly overestimate". No need for '(orange line)' etc in the text.

   Removed!

8. 295-296: "Figure 8 (c) shows the spatial distribution of the increments in the methane fluxes after the inversion (posterior-prior)". The word 'increment' normally implies a positive addition. Maybe better to refer to it as flux correction or adjustments

   Flux increments changed to flux correction.

9. 302 "trajectory of the river Yamuna and Ganges,". Trajectory may be replaced by 'course' or something more appropriate.

   Trajectory changed to course.

10. 303-305 "Several studies have shown rice cultivation as a key contributor to methane emissions here due to the use of nitrogen fertilizers, organic manure, and livestock population in this region [Singh et al., 2021]". Be generous with citations when you say 'several'.

    Several studies have shown rice cultivation as a key contributor to methane emissions here due to the use of nitrogen fertilizers, organic manure, and livestock population in this region [Singh et al., 2021].

    Changed to:

    Several studies have shown rice cultivation as a key contributor to methane emissions here (Anand et al., 2005; Gupta et al., 2015; Manjunath et al., 2006; Matthews et al., 1991) due to the use of nitrogen fertilizers, organic manure, and livestock population in this region (Singh et al., 2021)

11. 307-308 'In the area marked within the blue box,'. You should not be writing about the marked boxes, but specifically write Upper Indus Basin or whatever you can geographically name it

    In the area marked within the blue box, emission estimates are reduced by -2.4 Tg yr^{-1}

    Changed to:

    In the Upper Indus Basin (blue box), emission estimates are reduced by -2.4 Tg yr^{-1}

Conclusion

1. 419-420 "…the back box region…". This is not an appropriate reference to the analysis region in conclusion. Specify the region so that the conclusion stands alone.

   Within this increase, Bangladesh alone contributes +5.6 Tg yr-1, while the black-box region covering eastern India and Bangladesh accounts for +8.4 Tg yr^{-1} of the regional increment.

Changed to:

Within this increase, Bangladesh alone contributes +5.6 Tg yr-1, while the region covering eastern India and Bangladesh (black box) accounts for +8.4 Tg yr^{-1} of the regional increment.

2. "These analyses suggest that the 2020 rise in methane emissions is strongly linked to biogenic processes driven by glacial melt (in the Indus river basin), heavy monsoonal rainfall and enhanced inundation (both in the Indus river basin and in Bangladesh). These findings are consistent with earlier studies (e.g., Peng et al., (2022), Niwa et al., (2025)) that identify wetlands and agriculture as dominant contributors to the regional and global methane budget in recent years." Since you estimate only one year of emission, you do not need to tell from this particular study that there was a rise in 2020.

   Removed "2020"

3.2 Validation

To assess the robustness of the inversion results, we performed an independent validation using the GOSAT–TROPOMI blended XCH_4 dataset (Balasus et al., 2023). This relatively recent product combines TROPOMI and GOSAT XCH4 retrievals using a machine-learning bias-correction framework designed to reduce the systematic biases between the two satellite instruments relative to ground truth and to improve spatial consistency. The dataset is publicly available via AWS Open Data and has already been used in several studies to infer methane emissions. Importantly, it is developed independently of the WFMD TROPOMI retrievals used in our inversion, thereby providing a fully external and independent consistency check of the posterior solution.

Figure S1 shows the time series of domain averaged column mean methane concentrations for 2020, comparing the prior model simulation, the posterior model simulation, and the blended GOSAT–TROPOMI observations. The prior simulation systematically underestimates methane concentrations during the monsoon and post-monsoon months (Jun-Nov), while slightly overestimating concentrations during the pre-monsoon period (Jan-May). This behavior is consistent with the seasonal flux adjustments inferred by the inversion, where prior emissions were found to be too low in the second half of the year and too high in the first half. The posterior simulation shows a clear improvement in capturing both the seasonal amplitude and the temporal variability of the observations, although a slight overestimation is seen overall. In particular, the enhanced concentrations during August-October are much better reproduced after inversion, indicating that the additional emissions inferred during the monsoon season are physically consistent with the observed atmospheric signal.

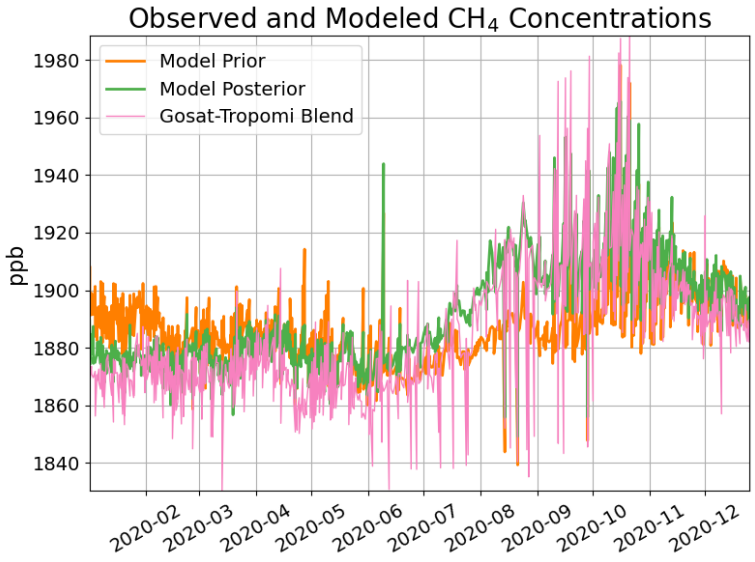

Figure S1. Domain-averaged prior and posterior modeled CH4 concentrations compared with the GOSAT–TROPOMI blended XCH_4 dataset.

3.2.1 Root Mean Square Error (RMSE) and Mean Bias Error (MBE)

The improvement is further quantified in Figure S2, which shows the (a) RMSE and (b) MBE between modeled and blended XCH_4 for three seasonal groupings: January–May, June–September, and October–December.

For January–May, the RMSE decreases from 15.94 ppb (prior) to 9.77 ppb (posterior), corresponding to a reduction of 6.18 ppb or 38.7%. During the monsoon season (June–September), where the largest seasonal mismatch was observed in the prior simulation, the RMSE decreases from 19.01 ppb to 12.07 ppb, representing a reduction of 6.93 ppb or 36.5%. This is the largest absolute RMSE improvement and confirms that the inversion effectively corrects the strong underestimation of methane during the monsoon period. For October–December, the improvement is smaller, with RMSE decreasing from 10.09 ppb to 9.86 ppb (a reduction of 0.24 ppb, or 2.3%), indicating that the prior simulation was already relatively consistent with observations during this period. Overall, the posterior simulation consistently reduces the error relative to the independent blended dataset, with the most pronounced improvements occurring during the monsoon season.

For January–May, the prior simulation shows a strong positive bias of +13.98 ppb, which is reduced to +7.07 ppb in the posterior simulation. This corresponds to a bias reduction of 6.91 ppb (~49% reduction), indicating that the inversion corrects the prior overestimation during the pre-monsoon season. During June–September, the prior simulation shows a pronounced negative bias of −10.49 ppb, reflecting the underestimation of emissions. After inversion, the bias shifts to +4.61 ppb, effectively correcting the sign of the bias and reducing its magnitude relative to the observations. For October–December, the prior bias is nearly neutral (−0.21 ppb), while the posterior shows a positive bias (+6.97 ppb). Although this increases the mean bias during this period, the RMSE remains largely unchanged, indicating that variability is still well represented.

Overall, the independent validation with the blended GOSAT–TROPOMI dataset demonstrates that the posterior solution improves both variance-based (RMSE) and mean-state (MBE) agreement with observations, increasing confidence in the inferred seasonal methane flux corrections.

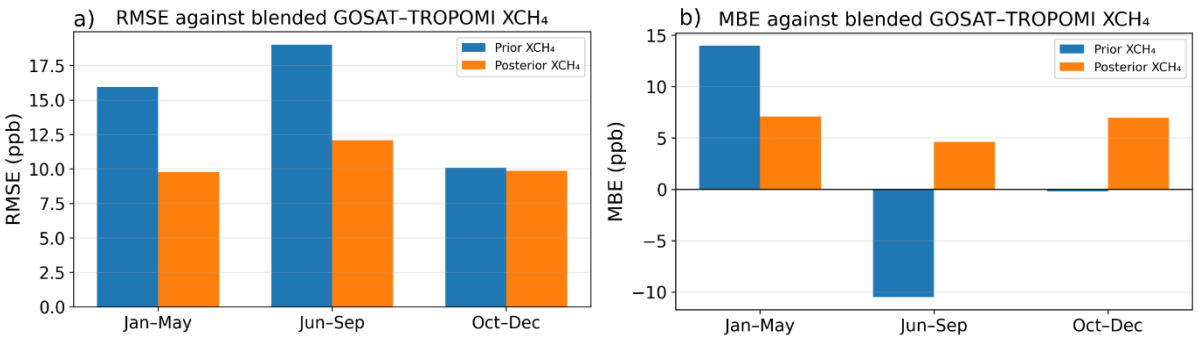

Figure S2. Seasonal RMSE (a) and MBE (b) of prior and posterior modeled XCH_4 relative to GOSAT–TROPOMI blended dataset. Statistics are shown for January–May, June–September, and October–December. Overall, the posterior simulation shows reduced errors and seasonal biases compared to the prior.

References

Anand, S., Dahiya, R. P., Talyan, V., and Vrat, P.: Investigations of methane emissions from rice cultivation in Indian context, Environment International, 31, 469–482, https://doi.org/10.1016/j.envint.2004.10.016, 2005.

Balasus, N., Jacob, D. J., Lorente, A., Maasakkers, J. D., Parker, R. J., Boesch, H., Chen, Z., Kelp, M. M., Nesser, H., and Varon, D. J.: A blended TROPOMI+GOSAT satellite data product for atmospheric methane using machine learning to correct retrieval biases, Atmospheric Measurement Techniques, 16, 3787–3807, https://doi.org/10.5194/amt-16-3787-2023, 2023.

Bovensmann, H., Burrows, J. P., Buchwitz, M., Frerick, J., Noël, S., Rozanov, V. V., Chance, K. V., and Goede, A. P. H.: SCIAMACHY: Mission Objectives and Measurement Modes, Journal of the Atmospheric Sciences, 56, 127–150, https://doi.org/10.1175/1520-0469(1999)056%253C0127:SMOAMM%253E2.0.CO;2, 1999.

Chen, A., Zhang, Z., Poulter, B., Feng, L., Liu, H., Murray, L. T., Yu, X., Huang, Z., Gaeta, D. C., Morgan, K. L., Zhu, Q., and Miller, S. M.: Spatial and Temporal Distribution of Global Wetland Methane Emissions During 2019–2020 Estimated From Satellite Observations, Journal of Geophysical Research: Atmospheres, 130, e2025JD044354, https://doi.org/10.1029/2025JD044354, 2025.

Dogniaux, M., Maasakkers, J. D., Girard, M., Jervis, D., McKeever, J., Schuit, B. J., Sharma, S., Lopez-Noreña, A., Varon, D. J., and Aben, I.: Global satellite survey reveals uncertainty in landfill methane emissions, Nature, 647, 397–402, https://doi.org/10.1038/s41586-025-09683-8, 2025.

Gupta, D. K., Bhatia, A., Kumar, A., Chakrabarti, B., Jain, N., and Pathak, H.: Global warming potential of rice (Oryza sativa)-wheat (Triticum aestivum) cropping system of the Indo-Gangetic Plains, Indian J Agri Sci, 85, 807–816, https://doi.org/10.56093/ijas.v85i6.49243, 2015.

Hu, H., Hasekamp, O., Butz, A., Galli, A., Landgraf, J., Aan de Brugh, J., Borsdorff, T., Scheepmaker, R., and Aben, I.: The operational methane retrieval algorithm for TROPOMI, Atmospheric Measurement Techniques, 9, 5423–5440, https://doi.org/10.5194/amt-9-5423-2016, 2016.

International Energy Agency(IEA): Methane and climate change – Methane Tracker 2021, 2021.

Jacob, D. J., Varon, D. J., Cusworth, D. H., Dennison, P. E., Frankenberg, C., Gautam, R., Guanter, L., Kelley, J., McKeever, J., Ott, L. E., Poulter, B., Qu, Z., Thorpe, A. K., Worden, J. R., and Duren, R. M.: Quantifying methane emissions from the global scale down to point sources using satellite observations of atmospheric methane, Atmospheric Chemistry and Physics, 22, 9617–9646, https://doi.org/10.5194/acp-22-9617-2022, 2022.

Jongaramrungruang, S., Matheou, G., Thorpe, A. K., Zeng, Z.-C., and Frankenberg, C.: Remote sensing of methane plumes: instrument tradeoff analysis for detecting and quantifying local sources at global scale, Atmospheric Measurement Techniques, 14, 7999–8017, https://doi.org/10.5194/amt-14-7999-2021, 2021.

Kuze, A., Suto, H., Nakajima, M., and Hamazaki, T.: Thermal and near infrared sensor for carbon observation Fourier-transform spectrometer on the Greenhouse Gases Observing Satellite for greenhouse gases monitoring, Appl. Opt., AO, 48, 6716–6733, https://doi.org/10.1364/AO.48.006716, 2009.

Liang, R., Zhang, Y., Chen, W., Zhang, P., Liu, J., Chen, C., Mao, H., Shen, G., Qu, Z., Chen, Z., Zhou, M., Wang, P., Parker, R. J., Boesch, H., Lorente, A., Maasakkers, J. D., and Aben, I.: East Asian methane emissions inferred from high-resolution inversions of GOSAT and TROPOMI observations: a comparative and evaluative analysis, Atmospheric Chemistry and Physics, 23, 8039–8057, https://doi.org/10.5194/acp-23-8039-2023, 2023.

Lindqvist, H., Kivimäki, E., Häkkilä, T., Tsuruta, A., Schneising, O., Buchwitz, M., Lorente, A., Martinez Velarte, M., Borsdorff, T., Alberti, C., Backman, L., Buschmann, M., Chen, H., Dubravica, D., Hase, F., Heikkinen, P., Karppinen, T., Kivi, R., McGee, E., Notholt, J., Rautiainen, K., Roche, S., Simpson, W., Strong, K., Tu, Q., Wunch, D., Aalto, T., and Tamminen, J.: Evaluation of Sentinel-5P TROPOMI Methane Observations at Northern High Latitudes, Remote Sensing, 16, 2979, https://doi.org/10.3390/rs16162979, 2024.

Lorente, A., Borsdorff, T., Butz, A., Hasekamp, O., aan de Brugh, J., Schneider, A., Wu, L., Hase, F., Kivi, R., Wunch, D., Pollard, D. F., Shiomi, K., Deutscher, N. M., Velazco, V. A., Roehl, C. M., Wennberg, P. O., Warneke, T., and Landgraf, J.: Methane retrieved from TROPOMI: improvement of the data product and validation of the first 2 years of measurements, Atmospheric Measurement Techniques, 14, 665–684, https://doi.org/10.5194/amt-14-665-2021, 2021.

Lorente, A., Borsdorff, T., Martinez-Velarte, M. C., and Landgraf, J.: Accounting for surface reflectance spectral features in TROPOMI methane retrievals, Atmos. Meas. Tech., 16, 1597–1608, https://doi.org/10.5194/amt-16-1597-2023, 2023.

Manjunath, K. R., Panigrahy, S., Kumari, K., Adhya, T. K., and Parihar, J. S.: Spatiotemporal modelling of methane flux from the rice fields of India using remote sensing and GIS, International Journal of Remote Sensing, 27, 4701–4707, https://doi.org/10.1080/01431160600702350, 2006.

Matthews, E., Fung, I., and Lerner, J.: Methane emission from rice cultivation: Geographic and seasonal distribution of cultivated areas and emissions, Global Biogeochemical Cycles, 5, 3–24, https://doi.org/10.1029/90GB02311, 1991.

Schneising, O., Buchwitz, M., Hachmeister, J., Vanselow, S., Reuter, M., Buschmann, M., Bovensmann, H., and Burrows, J. P.: Advances in retrieving XCH_4 and XCO from Sentinel-5 Precursor: improvements in the scientific TROPOMI/WFMD algorithm, Atmospheric Measurement Techniques, 16, 669–694, https://doi.org/10.5194/amt-16-669-2023, 2023.

Singh, A., Kuttippurath, J., Abbhishek, K., Mallick, N., Raj, S., Chander, G., and Dixit, S.: Biogenic link to the recent increase in atmospheric methane over India, Journal of Environmental Management, 289, 112526, https://doi.org/10.1016/j.jenvman.2021.112526, 2021.

Toha, M., Ariyan, T. N., and Alam, M.: Methane hotspots in landfills: A systematic review on transboundary dispersion and impacts on heatwaves in South Asia, Cleaner Waste Systems, 10, 100235, https://doi.org/10.1016/j.clwas.2025.100235, 2025.